Received: 19 July 2020 | Revised: 26 August 2020 | Accepted: 28 August 2020
DOI: 10.1002/pat.5102

RESEARCH ARTICLE

polymers advanced technologies WILEY

# The influence of structural and charge transport properties of PEDOT:PSS layers on the photovoltaic properties of polymer solar cells

A.K. Aimukhanov[1] | X.S. Rozhkova[1] | B.R. Ilyassov[2] | A.K. Zeinidenov[1] | N. Nuraje[2]

[1]Buketov University, Karaganda, Kazakhstan

[2]Department of Chemical and Materials Engineering, Nazarbayev University, Nur-Sultan, Kazakhstan

**Correspondence**
N. Nuraje, Department of Chemical and Materials Engineering
Nazarbayev University, 53 Kabanbay Batyr Avenue, Nur-Sultan 010000, Kazakhstan.
Email: nurxat.nuraje@nu.edu.kz

In this study, the effect of modification of poly(3,4-ethylenedioxythiophene):polystyrene sulfonate (PEDOT:PSS) morphology on its optical, charge transport, and photovoltaic properties of organic solar cells based on the P3HT:PC60BM bulk heterojunction is presented. It is shown that the addition of isopropyl alcohol to the PEDOT:PSS polymer solution and annealing of spin-coated PEDOT:PSS film leads to a change in its morphology, charge transport, and optical properties. By an impedance spectroscopy technique, the charge transport properties of PEDOT:PSS films were studied. It was established that the efficiency of carrier transport and the efficiency of the polymer solar cells depends on the structural features of PEDOT:PSS.

KEYWORDS
absorption and impedance spectroscopy, charge transfer, PEDOT:PSS, photovoltaic properties, polymer solar cells

## 1 | INTRODUCTION

Currently, the development of solar cells based on photoactive organic and polymer semiconductors is a promising and rapidly developing field. Polymer solar cells (PSCs) have the efficient charge separation at the phase boundary of the organic donor and acceptor materials, as well as the relatively high charge carrier mobility, which lead to the relatively high-power conversion efficiency (PCE) and can be assembled on a flexible substrate. The fabrication of PSCs is inexpensive and environmentally friendly, which will reduce the cost of the final product and simplify production processes compared to traditional crystalline materials and will allow to make large-scale production.[1,2]

The photoactive and semiconducting organic materials currently used in PSCs are extremely diverse in chemical nature. The goal of numerous studies in this still developing field is to create ordered molecular ensembles based on aromatic and heteroaromatic compounds with electron-donating and electron-withdrawing properties, capable of forming charge-transfer complexes that can intensively absorb the ultraviolet, visible, and infrared ranges of the solar spectrum. These materials are the basis of molecular electronics and organic photovoltaics (PV) with sufficiently optimal electrophysical and optical characteristics and long life span.[3,4]

The morphology of PSCs functional layers has a strong effect on PCE of devices. The formation of separate phases of the donor and acceptor components in the active layer, as well as their mutual ordering are very crucial. Optimal phase size and separation is necessary for both the separation of electrons and holes and for their efficient transport.[5] It is generally accepted that the domain size should be close to the mean free path of excitons in the active layer. By rough estimates, this value is 5 - 15 nm for polyconjugated polymers and can vary greatly depending on the purity of the materials and the crystallinity of the films. With a smaller domain size, the efficiency of charge separation can be great, but charge transport to the selective electrodes will be difficult, therefore, for each specific system there is an optimal fragmentation range. Charge transfer is severely affected if the formation of domains of more than 100 to 200 nm occurs.[5-7] In recent years, it has been convincingly proved that morphology of PCSs functional layers can have a decisive influence on the PCE of PCSs. The reason for this effect was the inhomogeneity of the active layer. When large donor nanoclusters are isolated from the acceptor, it strongly reduces the efficiency of photoinduced charge separation.[6] Thus, the main reason for the low values of PSCs performance is the tendency to aggregation and low solubility of active compounds, since the crystallization of the components in active layer leads to the formation of polycrystalline domains, which are characterized by undesirable large granularity and non-optimal crystalline ordering.[8,9] Moreover, the problems associated with the influence of the structural features of the other PSCs functional layers on fundamental parameters, such as the efficiency of charge carrier extraction with selective electrodes and the overall PCE are still not completely solved.

In the following works,[9-12] the authors have carried out studies on the effect of various solvents (methanol, ethanol, and isopropyl alcohol) on the characteristics of poly(3,4-ethylenedioxythiophene): polystyrene sulfonate (PEDOT:PSS) and the influence of modified PEDOT:PSS on PSCs efficiency. This work differs from mentioned studies by the investigation of charge transport mechanism in PEDOT:PSS films by impedance spectroscopy techniques.

In this study, the effect of the morphology and structural changes in the PEDOT:PSS film functioning as hole selective and transport layer on its optical and chare transport properties and on PV performance of PSCs has been investigated. The solution of PEDOT:PSS was diluted with a specific concentration of isopropyl alcohol in order to modify the morphology and structure of spin-coated PEDOT:PSS films. The improvement in the properties of the modified PEDOT:PSS films were determined by comparing the surface morphology, optical and impedance spectra (IS), efficiency and quantum efficiency (QE) of PSCs.

## 2 | EXPERIMENTAL

In this study the following reagents were used: PEDOT:PSS solution (1%, Ossila, Al 4083), Isopropyl alcohol (99.9%, Sigma-Aldrich, 3050 Spruce St Louis, MO 63103 United Statesh).

The chemical structure of the PEDOT:PSS compounds are shown in Figure 1. PEDOT:PSS films and PCSs were assembled on glass substrates coated with indium tin oxide (ITO). The cleaning of substrates was carried out according to the procedure described as mentioned in Reference 13. Before the spin-coating, the PEDOT:PSS solution was filtered through a 0.45 μm filter. PEDOT:PSS films were spin-coated at 5000 rpm (by a SPIN150i spin coater, Semiconductor Production System). After some films were annealed in air at a temperature of 120°C for 30 minutes. Then, 200 nm thick aluminum electrodes were deposited on a film surface in vacuum at a pressure of $10^{-5}$ Torr by Thermal Evaporating Coater (CY-1700x-spc-2, Zhengzhou CY Scientific Instruments Co., Ltd., Zhengzhou, China).

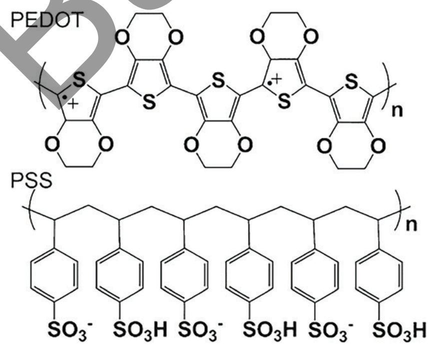

**FIGURE 1** Chemical structure of PEDOT and PSS. PEDOT, poly (3,4-ethylenedioxythiophene); PSS, polystyrene sulfonate

The PSCs were assembled by following procedures: the photoactive layer was spin-coated from chlorobenzene solution of P3HT:PC60BM (Borun New Material Technology Ltd., No.1158, jiangnan road, Ningbo, Zhejiang, China (Mainland)/315010) with concentration of 15.6:9.4 mg on the surface of PEDOT:PSS layer. After that, the samples were annealed in air at a temperature of 110°C for 10 minutes. Then an aluminum electrode was deposited onto the surface of photoactive layers by the thermal evaporation in high vacuum. Finally, devices were encapsulated by epoxy and glass slides.

The surface topography of the samples was studied by a high-resolution atomic force microscope (AFM) JSPM-5400 (JEOL, Tokyo, Japan). To process the images obtained by AFM, a Win SPMII Data-Processing Software for analyzing scanning probe microscopy data was used. Roughness of PEDOT:PSS thin films were analyzed from AFM image data.

The absorption spectra of samples were recorded by an AvaSpec-ULS2048CL-EVO spectrometer (Avantes), which measures absorption spectra in the range of 200 to 1100 nm and has an optical resolution of 0.04 nm.

The IS of the devices were measured by a potentiostat with the FRA32 impedance module (P45X, Elins) described in detail as mentioned in Reference 14, and fitting of IS was performed by Electrochemical Impedance Spectroscopy analyzer software (EIS-analyzer).

The PV performance of PSCs was measured by PVIV-1A I-V Test Station under a Sol3A Class AAA Solar Simulator illumination (Newport). The QE spectrum was measured by a Newport IQE200 setup.

## 3 | RESULTS AND DISCUSSION

We have prepared two different types PEDOT:PSS films. The first PEDOT:PSS films were coated from standard PEDOT:PSS solution (further they will be mentioned as standard-PEDOT:PSS or s-PEDOT:PSS). The second PEDOT:PSS films were coated from a diluted PEDOT:PSS solution (further they will be mentioned as modified PEDOT:PSS or m-PEDOT:PSS). Both types of PEDOT:PSS were used without and with annealing.

The AFM images of the surface morphology of the PEDOT:PSS films are shown in Figure 2. From Figure 2A, it can be seen that the unannealed s-PEDOT:PSS film has a granular structure. In the background of a fine granular structure, large particles are observed and the surface roughness is $R_a$ = 2.41 nm (arithmetic mean deviation of the assessed surface) according to AFM data. After thermal annealing

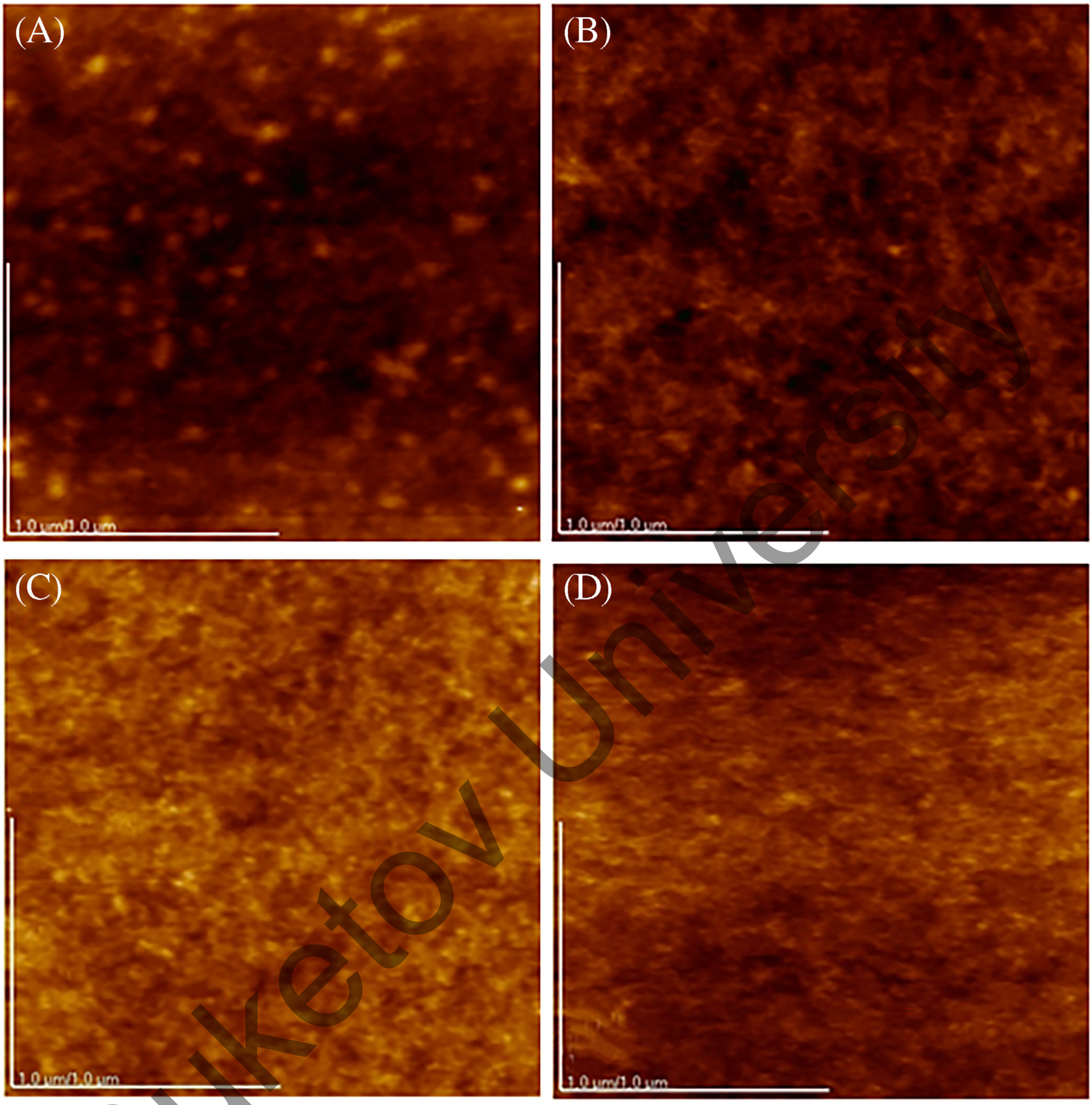

**FIGURE 2** Atomic force microscopic images of the surface morphology of PEDOT:PSS films. A, s-PEDOT:PSS without annealing. B, s-PEDOT:PSS with annealing. C, m-PEDOT:PSS without annealing. D, m-PEDOT:PSS with annealing. PEDOT:PSS, poly (3,4-ethylenedioxythiophene):polystyrene sulfonate

of s-PEDOT:PSS film at a temperature of 120°C, the portion of large particles (Figure 2B) significantly decreases, and the roughness becomes $R_a$ = 1.14 nm. When isopropyl alcohol is added to PEDOT:PSS solution, the surface topography of modified PEDOT:PSS film improves. As it can be seen from Figure 2C, modified PEDOT:PSS film reveals a better surface smoothing and the absence of large particles. The roughness in this case becomes $R_a$ = 0.94 nm. Thermal annealing of the modified film at a temperature of 120°C leads to greater degree of uniformity of the surface of the PEDOT:PSS film (Figure 2D), the roughness of which is $R_a$ = 0.76 nm. Table 1 shows the roughness values of the PEDOT:PSS films.

The absorption spectra of PEDOT:PSS films are represented in Figure 3. It can be seen from the figure that the film of the unannealed s-PEDOT:PSS has a maximum $D_1$ at a wavelength of $\lambda_1$ = 228.7 nm with a half-width of the spectrum (FHWM) of 46 nm (Figure 3, curve 1). In the absorption spectra of all films, the shoulder

**TABLE 1** The surface roughness of the films PEDOT:PSS

| Samples | $R_a$ (nm) |
|---|---|
| Standard PEDOT:PSS without annealing | 2.41 ± 0.002 |
| Standard PEDOT:PSS with annealing | 1.14 ± 0.002 |
| Modified PEDOT:PSS without annealing | 0.94 ± 0.002 |
| Modified PEDOT:PSS with annealing | 0.76 ± 0.002 |

Abbreviation: PEDOT:PSS, poly(3,4-ethylenedioxythiophene):polystyrene sulfonate.

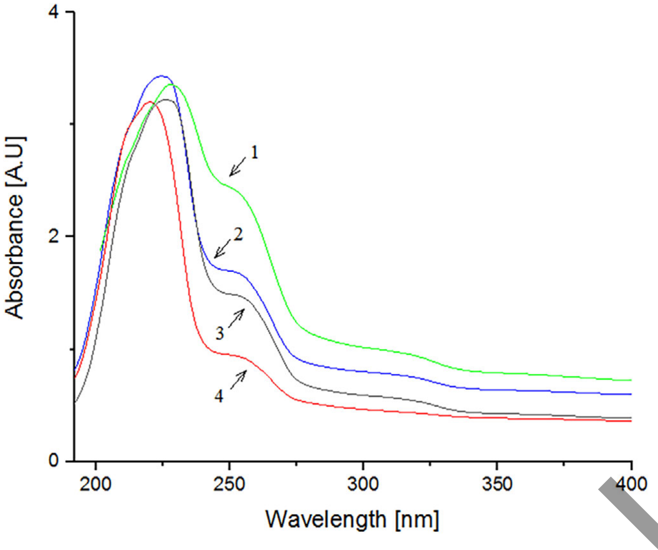

**FIGURE 3** Absorption spectra of the standard and modified PEDOT:PSS films. 1, Film of the s-PEDOT:PSS without annealing. 2, Annealed film of the s-PEDOT:PSS. 3, Film of the m-PEDOT:PSS without annealing. 4, Annealed film m-PEDOT:PSS. PEDOT:PSS, poly (3,4-ethylenedioxythiophene):polystyrene sulfonate

with a maximum $D_2$ at $\lambda_2$ = 252.5 nm is observed, which is associated with the absorption of the aromatic PSS fragment.[15] After annealing, the maximum absorption of s-PEDOT:PSS film ($\lambda_1$) is shifted to 224.7 nm, and the half-width decreased and amounted to 37 nm. Also, a decrease in the absorption $D_2$ of the aromatic fragment of PSS (Figure 3, curve 2) is observed.

When isopropyl alcohol is added to the PEDOT:PSS solution, the absorption maximum ($\lambda_1$) of the film remains almost unchanged at 224.6 nm, the FWHM is 35 nm, but the intensity of the absorption of the aromatic fragment of PSS decreases (Figure 3, curve 3). After subsequent annealing of the modified PEDOT:PSS film, a shift of the $\lambda_1$ maximum to the short-wavelength region to 220.3 nm is observed, the half-width of the spectrum decreases to 33 nm, and the intensity of the PSS absorption also decreases (Figure 3, curve 4). Table 2 shows the characteristics of the absorption spectra of PEDOT:PSS films.

It is known that, due to its hydrophobicity, the PEDOT polymer is not soluble in isopropyl alcohol; in turn, PSS has a high degree of hydrophilicity.[16] It was shown as mentioned in Reference 10 that the addition of methanol to the PEDOT:PSS film leads to a decrease in the intensity of absorption spectrum of the aromatic fragment of PSS. The authors of the work suggested that this effect can be observed using a wide class of solvents. According to literature, agglomerates are found to be PSS-rich region. PSS content is isolator and the regions which have this PSS-rich agglomerates impede charge transfer. So, to obtain high-effective PEDOT:PSS based devices, it is needed to get uniform PEDOT:PSS films with less PSS-rich regions.

The observed changes in the absorption spectra of the films are related to the structural features of PEDOT:PSS. Initially, the untreated film has large agglomerates and in the optical spectrum there is intense absorption of the aromatic fragment of PSS. After thermal annealing, the density of large agglomerates decreases and the intensity of the absorption band of PSS lessens. Adding isopropyl

**TABLE 2** Spectral characteristics of PEDOT:PSS films

| | Adsorption Peak | | | | |
|---|---|---|---|---|---|
| Samples | $\lambda_1$ (nm) | $\lambda_2$ (nm) | $D_1$ | $D_2$ | FWHM (nm) |
| Standard PEDOT:PSS | 228.7 ± 0,07 | 252.5 ± 0.07 | 3.35 ± 0.004 | 2.5 ± 0.004 | 46 |
| Annealed standard PEDOT:PSS | 224.7 ± 0,07 | 252.5 ± 0.07 | 3.45 ± 0.004 | 1.9 ± 0.004 | 37 |
| Modified PEDOT:PSS | 224.6 ± 0,07 | 252.5 ± 0.07 | 3.21 ± 0.004 | 1.4 ± 0.004 | 35 |
| Annealed modified PEDOT:PSS | 220.3 ± 0,07 | 252.5 ± 0.07 | 3.19 ± 0.004 | 1 ± 0.004 | 33 |

Abbreviations: FWHM, full width at half maximum; PEDOT:PSS, poly(3,4-ethylenedioxythiophene):polystyrene sulfonate.

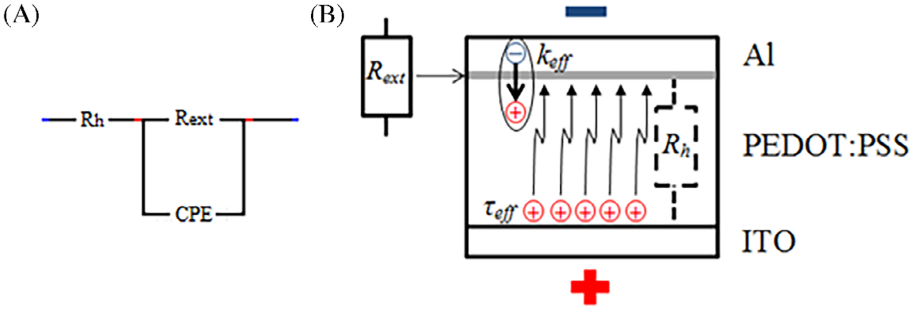

**FIGURE 4** A, Equivalent electrical circuit. B, Charge transfer mechanism in ITO/PEDOT:PSS/Al cell. PEDOT:PSS, poly(3,4-ethylenedioxythiophene): polystyrene sulfonate

alcohol to PEDOT:PSS solution leads to forming agglomerates free uniform and smooth PEDOT:PSS films with the reduced intensity of the absorption band of the PSS aromatic fragment. Thus, annealing and the addition of isopropyl alcohol leads to the structural change of PEDOT:PSS and according to the agglomerates loss and decrease in absorption band of the PSS aromatic rings, it is reasonable to conclude that PSS is removed from the film surface.

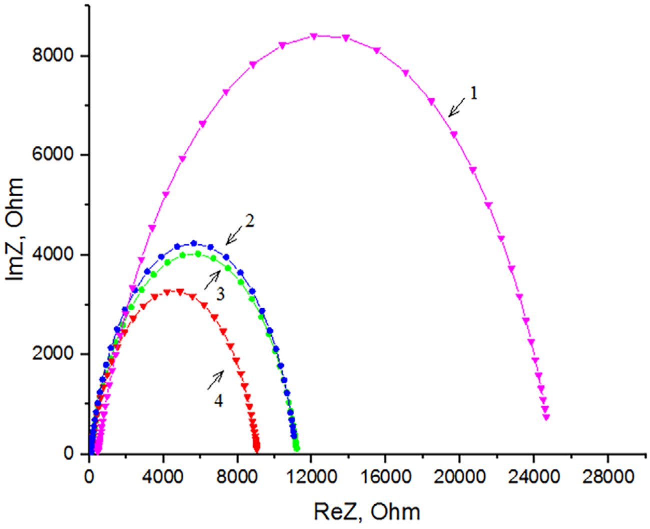

**FIGURE 5** The impedance spectra of ITO/PEDOT:PSS/Al cells measured at voltage parameters of −500 mV and frequencies from 100 kHz to 0.5 Hz: 1, s-PEDOT:PSS. 2, Annealed s-PEDOT:PSS. 3, m-PEDOT:PSS. 4, Annealed m-PEDOT:PSS. ITO, indium tin oxide; PEDOT:PSS, poly(3,4-ethylenedioxythiophene):polystyrene sulfonate

The IS of ITO/PEDOT:PSS/Al cells were measured. The analysis of impedance data was carried out according to the diffusion-recombination model, and the equivalent circuit shown in Figure 4A was used for the fitting.[17] Charge transport and transfer mechanism in ITO/PEDOT:PSS/Al cell is shown in Figure 4B. The IS of ITO/PEDOT:PSS/Al cells based on the s-PEDOT:PSS and m-PEDOT:PSS are shown in Figure 5. The IS were fitted using the EIS-analyzer software, and the main charge transport parameters of the films were calculated (Table 3): where: $k_{eff}$ is the effective charge carrier extraction rate from PEDOT:PSS, $\tau_{eff}$ is the effective transit time through PEDOT:PSS, $R_h$ is the PEDOT:PSS film resistance, and $R_{ext}$ is the transfer resistance of charge carriers at the PEDOT:PSS/electrode interface associated with the extraction of charge carriers from PEDOT:PSS.

Charge transport parameters determined form IS data are represented in Table 3. As it can be seen from Table 3, annealing and the addition of isopropyl alcohol significantly affect the resistance of the PEDOT:PSS film ($R_h$) and the transfer resistance at the PEDOT:PSS/electrode interface ($R_{ext}$). The resistance of the unannealed s-PEDOT:PSS has the highest value; further annealing at a temperature of 120°C leads to a decrease in the resistance by more two times. The addition of isopropyl alcohol to the PEDOT:PSS solution leads to the formation of m- PEDOT:PSS film with a resistance of two times less than the resistance of s-PEDOT:PSS film. However, further annealing only slightly reduces the resistance of the m-PEDOT:PSS film. Lower resistance of m- PEDOT:PSS film should improve the solar cell current and generally increase PV performance.

A similar dynamics is observed in the change of the charge transfer resistance at the PEDOT:PSS/electrode interface ($R_{ext}$). $R_{ext}$ is also

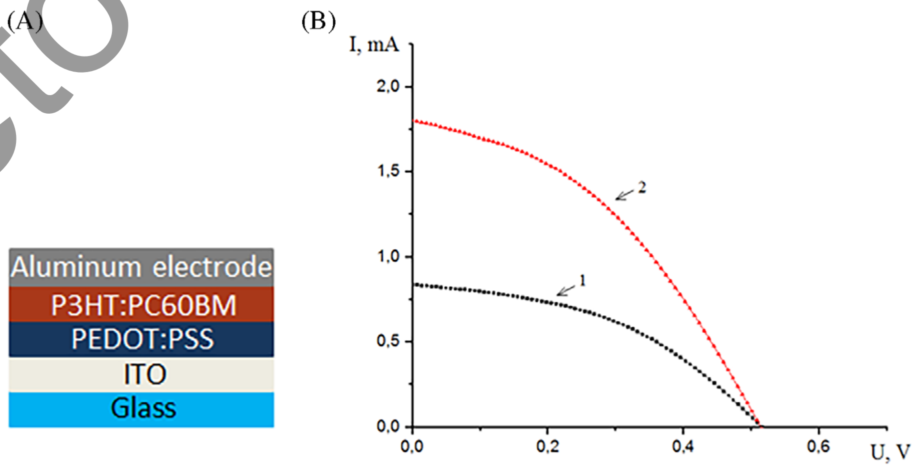

**FIGURE 6** A, Schematic representation of organic solar cell. B, Current-voltage characteristic of organic solar cells. 1, Cell with s-PEDOT:PSS. 2, Cell with m-PEDOT:PSS. PEDOT:PSS, poly(3,4-ethylenedioxythiophene):polystyrene sulfonate

**TABLE 3** The charge transport parameters of the films

| Samples | $R_h$ (Ohm) | $R_{ext}$ (Ohm) | $k_{eff}$ ($s^{-1}$) | $\tau_{eff}$ (ms) |
|---|---|---|---|---|
| s-PEDOT:PSS | 145.9 | 24 532 | 44.3 | 22.57 |
| Annealed s-PEDOT:PSS | 65.5 | 11 097 | 56.8 | 17.61 |
| m-PEDOT:PSS | 66.2 | 11 161 | 92.5 | 10.81 |
| Annealed m-PEDOT:PSS | 63.7 | 9010,6 | 93.5 | 10.70 |

Abbreviation: PEDOT:PSS, poly(3,4-ethylenedioxythiophene):polystyrene sulfonate.

**TABLE 4** Photovoltaic performance of organic solar cells

| Samples | $U_{oc}$ (V) | $J_{sc}$ (mA/cm$^2$) | $U_{max}$ (V) | $J_{max}$ (mA/cm$^2$) | FF | PCE (%) |
|---|---|---|---|---|---|---|
| s-PEDOT:PSS/P3HT:PC60BM/Al | 0.51 | 6.5 | 0.3 | 4.69 | 0.42 | 1.42 |
| m-PEDOT:PSS/P3HT:PC60BM/Al | 0.51 | 11.19 | 0.3 | 7.75 | 0.41 | 2.34 |

Abbreviations: FF, fill factor; PCE, power conversion efficiency; PEDOT:PSS, poly(3,4-ethylenedioxythiophene):polystyrene sulfonate.

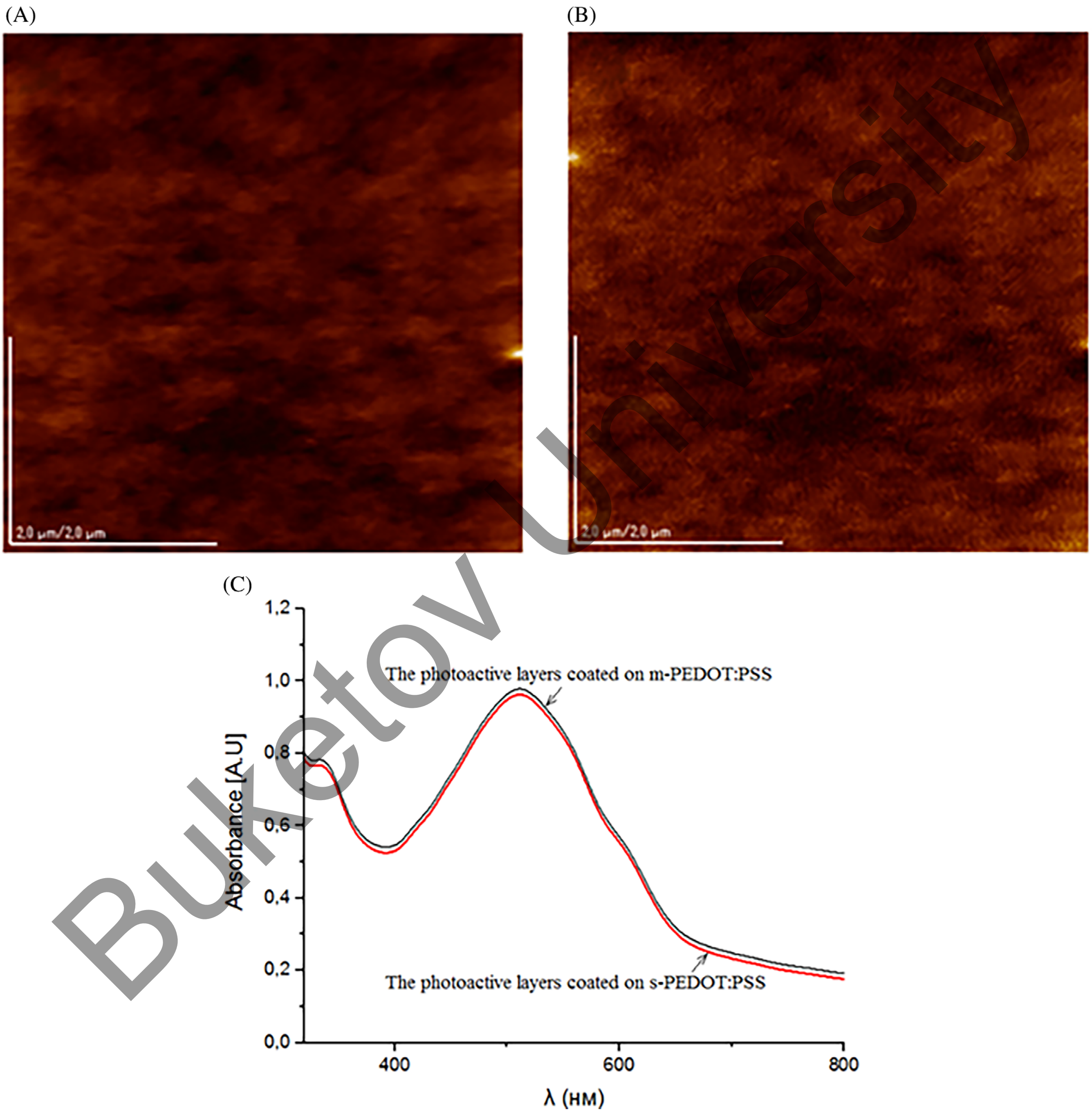

**FIGURE 7** A, Atomic force microscopic images of the surface morphology of photoactive layer with s-PEDOT:PSS. B, Atomic force microscopic images of the surface morphology of photoactive layer with m-PEDOT:PSS. C, UV-VIS absorbance spectra. PEDOT:PSS, poly (3,4-ethylenedioxythiophene):polystyrene sulfonate

larger for the unannealed s-PEDOT:PSS film. Upon further annealing, $R_{ext}$ decreases by more than two times. As in the case of $R_h$, when isopropyl alcohol is added to the original solution, $R_{ext}$ is halved. With further annealing, $R_{ext}$ decreases by almost 20%. $R_{ext}$ affects the efficiency of charge extraction rate from PEDOT:PSS films, and the lower value of $R_{ext}$ should lead to the greater value of efficiency of accumulation of charge carriers and photocurrents of solar cells.

The $k_{eff}$ and $\tau_{eff}$ characterize the rate of the extraction of charge carriers from PEDOT:PSS film and the effective transit time of charge carriers in PEDOT:PSS. As can be seen from Table 3, the annealing of the films slightly affects $k_{eff}$ and $\tau_{eff}$, however, there is a positive dynamics. However, the addition of isopropyl alcohol to the original solution has a noticeable positive trend for $k_{eff}$ and $\tau_{eff}$. The extraction rate of charge carriers from m-PEDOT:PSS increased approximately twofold, and the effective transit time of charge carriers decreased inversely indicating faster charge transport. At a bias applied according to the Figure 4B, holes are injected into PEDOT:PSS from ITO and diffuse to the Al electrode, where they recombine with electrons. The fast transport of injected holes to the external electrode is very important, since it reduces the probability of their reverse recombination. In our case, fast hole transport is ensured by improving the morphology and structure of PEDOT:PSS after adding isopropyl alcohol to the original solution, which also leads to an improvement in the quality of the PEDOT:PSS/electrode interface.

Then the annealed films of the standard and modified PEDOT:PSS were used as hole selective electrodes for PSCs based on P3HT:PC60BM bulk heterojunction (Figure 6A). The scheme and current-voltage characteristic of the assembled organic cells are shown in Figure 6.

The PV performance of PSCs is shown in Table 4, where $J_{max}$ and $U_{max}$ are the maximum values of current and voltage, $U_{oc}$ is the open circuit voltage, $J_{sc}$ is the short-circuit current density, FF is the fill factor, and PCE. The FF and PCE of PSCs were determined according to the procedure described as mentioned in Reference 18.

As can be seen from Table 4, the open circuit voltage ($U_{oc}$) of devices, both with the s-PEDOT:PSS and with the m-PEDOT:PSS, is the same, since voltage is determined by the energy of the P3HT and PC60BM. The short-circuit current density ($J_{sc}$) generated by cells with a m-PEDOT:PSS is almost 1.7 times higher than current density of cells based on the s-PEDOT:PSS. Both types of solar cells were obtained under the same conditions and, therefore, a significant difference in current is explained by the structural features and properties of PEDOT:PSS. The AFM topographies and UV-VIS absorbance spectra of the photoactive layers coated on both types of PEDOT:PSS are shown in Figure 7 and there are no significant differences as in morphology (Figure 7A,B) and in optical absorbance spectra (Figure 7C) of photoactive layers, which indicate that differences in PV performance are attributed only with the modification of PEDOT:PSS layer and PEDOT:PSS/photoactive interface. The structure of the modified PEDOT:PSS provides faster injection and transport of holes to the external electrode (ITO), which reduces the probability of hole recombination with electrons in the PC60BM and boosts the efficiency of hole accumulation on the external electrode. All of the above increases the photocurrent of the cell and, as a result, PCE of the cell with the modified PEDOT:PSS is more than 1.6 times higher than PCE of the cell with the s-PEDOT:PSS.

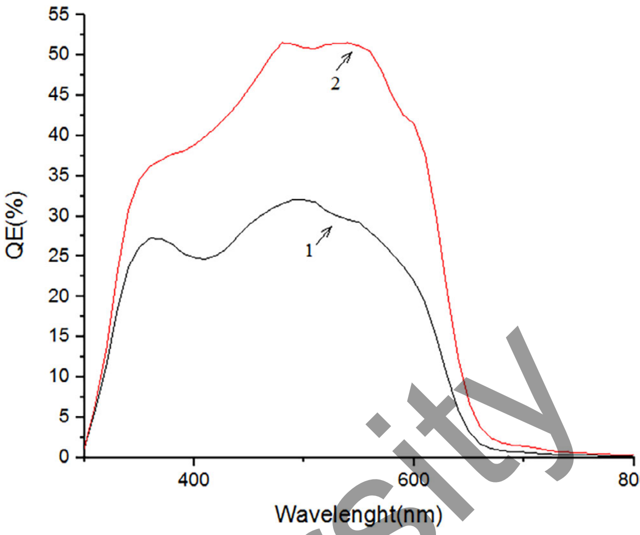

**FIGURE 8** Quantum efficiency (QE) of organic solar cells: 1, QE of cells with the s-PEDOT:PSS. 2, QE of cells with m-PEDOT:PSS. PEDOT:PSS, poly(3,4-ethylenedioxythiophene):polystyrene sulfonate

The QE of both type solar cells are presented in Figure 8. The pattern of spectral sensitivity for both cells based on s-PEDOT:PSS and m-PEDOT:PSS is almost identical and corresponds to typical devices with PEDOT:PSS/P3HT:PC60BM/Al configuration. However, the values of QE in the spectral range of 350 to 650 nm differ significantly. As can be seen from the figure, the QE of the cell with the s-PEDOT:PSS in the indicated range does not exceed 31.5%, and for the cell with the m-PEDOT:PSS reaches 51.6%. A significant improvement in the QE of m-PEDOT:PSS based cell correlates with the *I-V* curve and IS data, and indicates that a modified PEDOT:PSS with improved morphology and structure more efficiently extracts and transports holes to the ITO electrode.

## 4 | CONCLUSIONS

Inorder to conlude, it was found that thermal annealing and the addition of isopropyl alcohol to the PEDOT:PSS solution lead to an improvement in the morphology and structure of spin-coated PEDOT:PSS films. According to AFM images and data, modified PEDOT:PSS films have better surface morphology, more uniform and smooth. In the optical absorption spectrum of the modified PEDOT:PSS films, a decrease in the intensity of the absorption band due to the aromatic fragment of PSS is observed, which indicates structural changes in the PEDOT:PSS film. It was shown that the structural features of PEDOT:PSS affect the charge transport properties of films. It was established that the modification of the structure of the PEDOT:PSS layer improves the charge transport properties, which leads to enhancing the short circuit current density by 1.7 times, and PCE and QE of cells by 1.6 times.

## ACKNOWLEDGEMENT

This work was supported by the grant of Buketov University.

## CONFLICT OF INTEREST

The authors declare no potential conflict of interest.

## ORCID

*X.S. Rozhkova* https://orcid.org/0000-0003-3048-6171

*N. Nuraje* https://orcid.org/0000-0002-4335-8905

## REFERENCES

1. Huang YF, Inigo AR, Chang CC, et al. Nanostructure-dependent vertical charge transport in MEH-PPV films. *Adv Funct Mater*. 2007;17(15):2902-2910.
2. Sommeling PM, Spath M, Roosmalen JAM, Meyer TB, Meyer AF, Kohle O. Dye-sensitized Nanocrystalline TiO2 solar cells on flexible substrates. Paper presented at: *Proceedings of the 2nd World Conference and Exhibition on Photovoltaic Solar Energy Conversion*; July 6–10, 1998; Vienna, Austria. http://citeseerx.ist.psu.edu/viewdoc/download?doi=10.1.1.424.2530&rep=rep1&type=pdf.
3. Soga T. *Nanostructured Materials for Solar Energy Conversion*. Nagoya, Japan: Elsevier; 2006:614.
4. Zou T, Wang X, Ju H, Zhao L, Guo T, Wu W, Wang H. Controllable molecular packing motif and overlap type in organic nanomaterials for advanced optical properties. *Crystals* 2018; 8(1)22: 1–12.
5. Hoppe H, Sariciftci NS. Morphology of polymer/fullerene bulk heterojunction solar cells. *J Mater Chem*. 2006;16:45-61.
6. Hoppe H, Sariciftci NS. Organic solar cells: an overview. *J Mater Res*. 2004;19:1924-1945.
7. Coakley KM, McGehee MD. Conjugated polymer photovoltaic cells. *Chem Mater*. 2004;16:4533-4542.
8. Ma W, Yang C, Gong X, Lee K, Heeger AJ. Thermally stable, efficient polymer solar cells with nanoscale control of the interpenetrating network morphology. *Adv Funct Mater*. 2005;15:1617-1622.
9. Namkoong G, Younes EM, Abdel-Fattah TM, El-Maghraby EM, Elsayed AH, Abo Elazm AH. Aging process of PEDOT:PSS dispersion and robust recovery of aged PEDOT: PSS as a hole transport layer for organic solar cells. *Org Electron*. 2015;25:1199-1566.
10. Alemu D, Wei HY, Ho KC, Chu CW. Highly conductive PEDOT:PSS electrode by simple film treatment with methanol for ITO-free polymer solar cells. *Energy Environ Sci*. 2012;5:9662-9671.
11. Chang SH, Chen WN, Chen CC, et al. Wu CG. Manipulating the molecular structure of PEDOT chains through controlling the viscosity of PEDOT:PSS solutions to improve the photovoltaic performance of CH3NH3PbI3 solar cells. *Sol Energy Mater Sol Cells*. 2016;161:7-13.
12. Pali LS, Jindal R, Garg A. Screen printed PEDOT:PSS films as transparent electrode and its application in organic solar cells on opaque substrates. *J Mater Sci Mater Electron*. 2018;29(13):11030-11038.
13. Kim K, Ihm K, Kim B. Surface property of indium tin oxide (ITO) after various methods of cleaning. *Acta Phys Pol A*. 2015;127(4):1176-1179.
14. Bisquert J, Mora-Sero I, Fabregat-Santiago F. Diffusion–recombination impedance model for solar cells with disorder and nonlinear recombination. *ChemElectroChem*. 2014;1(1):289-296.
15. Xia Y, Sun K, Ouyang J. Highly conductive poly(3,-4-ethylenedioxythiophene):poly(styrene sulfonate) films treated with an amphiphilic fluoro compound as the transparent electrode of polymer solar cells. *Energy Environ Sci*. 2012;5:5325-5332.
16. Kim YH, Sachse C, Machala ML, May C, Muller-Meskamp L, Leo K. Highly conductive PEDOT:PSS electrode with optimized solvent and thermal post-treatment for ITO-free organic solar cells. *Adv Funct Mater*. 2011;21:1076-1081.
17. Yuan X, Song C, Wang H, Zhang J, 2010. *EIS Equivalent Circuits in Electrochemical Impedance Spectroscopy in PEM Fuel Cells*. London, England:Springer-Verlag; 2010. 420 p.
18. Khanam JJ, Foo SY. Modeling of high-efficiency multi-junction polymer and hybrid solar cells to absorb infrared light. *Polymers*. 2019;11(2):383.

**How to cite this article:** Aimukhanov AK, Rozhkova XS, Ilyassov BR, Zeinidenov AK, Nuraje N. The influence of structural and charge transport properties of PEDOT:PSS layers on the photovoltaic properties of polymer solar cells. *Polym Adv Technol*. 2021;32:497–504. https://doi.org/10.1002/pat.5102